Received: 25 February 2019 | Revised: 29 May 2019 | Accepted: 5 June 2019

DOI: 10.1002/hbm.24789

RESEARCH ARTICLE

WILEY

Mapping hemispheric asymmetries of the macaque cerebral cortex during early brain development

Jing Xia[1,2] | Fan Wang[2] | Zhengwang Wu[2] | Li Wang[2] | Caiming Zhang[1] | Dinggang Shen[2,3] | Gang Li[2]

[1]Department of Computer Science and Technology, Shandong University, Jinan, Shandong, China

[2]Department of Radiology and BRIC, University of North Carolina at Chapel Hill, Chapel Hill, North Carolina

[3]Department of Brain and Cognitive Engineering, Korea University, Seoul, Republic of Korea

Correspondence
Jing Xia, Department of Computer Science and Technology, Shandong University, Shandong, China.
Email: xiajing0904@gmail.com

Dinggang Shen and Gang Li, Department of Radiology and BRIC, University of North Carolina at Chapel Hill, UNC-CH School of Medicine, MRI Building, CB #7513, 106 Mason Farm Road, Chapel Hill, NC 27599.
Email: dgshen@med.unc.edu; gang_li@med.unc.edu

Abstract

Studying cortical hemispheric asymmetries during the dynamic early postnatal stages in macaque monkeys (with close phylogenetic relationship to humans) would increase our limited understanding on the possible origins, developmental trajectories, and evolutional mechanisms of brain asymmetries in nonhuman primates, but remains a blind spot to the community. Via cortical surface-based morphometry, we comprehensively analyze hemispheric structural asymmetries in 134 longitudinal MRI scans from birth to 20 months of age from 32 healthy macaque monkeys. We reveal that most clusters of hemispheric asymmetries of cortical properties, such as surface area, cortical thickness, sulcal depth, and vertex positions, expand in the first 4 months of life, and evolve only moderately thereafter. Prominent hemispheric asymmetries are found at the inferior frontal gyrus, precentral gyrus, posterior temporal cortex, superior temporal gyrus (STG), superior temporal sulcus (STS), and cingulate cortex. Specifically, the left planum temporale and left STG consistently have larger area and thicker cortices than those on the right hemisphere, while the right STS, right cingulate cortex, and right anterior insula are consistently deeper than the left ones, partially consistent with the findings in human infants and adults. Our results thus provide a valuable reference in studying early brain development and evolution.

KEYWORDS

cortical development, cortical thickness, hemispheric asymmetries, macaque monkeys

1 | INTRODUCTION

Nonhuman primates, especially macaque monkeys, are a highly valuable and widely used animal model for human neuroscience studies, due to their close phylogenetic relationship to human (Rilling, 2014). In neuroimaging studies of *human* brains, hemispheric asymmetries were found in a set of cortical features (Dubois et al., 2010), such as sulcal depth (Davatzikos & Bryan, 2002; Li et al., 2013; Ochiai et al., 2004; Van Essen, 2005), surface area (Li et al., 2013; Lyttelton et al., 2009), cortical thickness (Hamilton et al., 2007; Luders et al., 2005; Shaw et al., 2009), and vertex position (Li et al., 2013; Lyttelton et al., 2009; Thompson et al., 1998; Van Essen, Glasser, Dierker, Harwell, & Coalson, 2011). Among these cortical features, cortical thickness and surface area are important and distinct properties of cortical structures and they are related to normal development and aging, functions, and behaviors (Bogart et al., 2012; Scott et al., 2016). Sulcal depth is an important measurement of cortical folding degree, which could help us better understand cortical folds and related functions (Bogart et al., 2012). Vertex position is the 3D coordinate of a vertex on the surface mesh representation of the cortex, and the local relationship of cortical

vertices reflects the shape of the cortex. The hemispheric asymmetries (i.e., the relative offsets) of vertex position can provide important information on cortical shape and positional asymmetries between right and left hemispheres. Many of these asymmetries were originally presumed to support unique human characteristics such as language and handedness (Rilling, 2014). Studying the corresponding hemispheric asymmetries of these distinct features in nonhuman primates could increase the likelihood of identifying the antecedent conditions for homologous lateralized functions in human (Hopkins, Misiura, Pope, & Latash, 2015) and help us better understand the evolution of special features in human brains (Rilling, 2014).

In fact, neuroimaging studies of *nonhuman primates* have shown that certain hemispheric asymmetries found in human brains are also present in chimpanzees (Gannon, Holloway, Broadfield, & Braun, 1998; Hopkins et al., 2017; Lyn et al., 2011) and Old World monkeys, such as baboons (Marie et al., 2017) and macaque monkeys (Bogart et al., 2012). For instance, the left inferior frontal gyrus (IFG) and left planum temporale (PT), which are involved in language production and comprehension skills in human (Bogart et al., 2012), have been shown larger and deeper than those on the right hemisphere in chimpanzees and baboons (Gannon et al., 1998; Hopkins, Marino, Rilling, & MacGregor, 1998; Lyn et al., 2011; Marie et al., 2017), similar to the findings in human infants, old children, and adults (Glasel et al., 2011; Hill et al., 2010; Li, Nie, Wang, et al., 2012). The right superior temporal sulcus (STS) has been shown larger than the left STS in adult macaque monkeys (Bogart et al., 2012), similar to the findings in human brains (Benkarim et al., 2017; Clouchoux et al., 2012; Dubois, 2015), where right-deeper-than-left asymmetry in the STS has been found from later fetal stage to adulthood (Dubois et al., 2007; Van Essen et al., 2011).

Like human brains, macaque monkey brains also exhibit dynamic development during early postnatal years (Malkova, Heuer, & Saunders, 2006). Many hemispheric asymmetries in human brains are largely established during perinatal stages and further evolve moderately during postnatal brain development (Dubois et al., 2007; Glasel et al., 2011; Li, Nie, Wang, et al., 2012; Toga & Thompson, 2015). Therefore, studying hemispheric asymmetries in macaque monkeys during early postnatal stages would increase our very limited understanding on the possible origins (Muntané et al., 2017), developmental trajectories, and mechanisms of brain asymmetries in macaque monkeys (Scott et al., 2016), as well as their evolutional changes from macaque to human (Hill et al., 2010; Rilling, 2014). Moreover, this could also provide a valuable reference in the studies of many neurodevelopmental disorders that exhibit abnormal hemispheric asymmetries, such as autism (Bauman et al., 2013; Watson & Platt, 2012) and schizophrenia (Hamilton et al., 2007; Lewis, 1997), especially with the increasing availability of macaque models of neurodevelopmental disorders (Chen et al., 2017; Niu, Li, & Ji, 2017).

However, due to difficulties in analyzing the brain MRI data of macaque monkeys during infancy, which typically exhibits low tissue contrast and dynamic imaging appearance as in human infants (Wang et al., 2018), our knowledge remains scarce on the spatiotemporal changes of hemispheric structural asymmetries in macaque brains during early postnatal stages (Bogart et al., 2012; Gannon, Kheck, & Hof, 2008). To fill this knowledge gap, by leveraging an infant-dedicated computational pipeline (Wang et al., 2018), we perform cortical surface-based morphometry on longitudinal MRI data from a public rhesus macaque neurodevelopment dataset with 134 scans from 32 macaques (Young et al., 2007). Thus, this study provides the first comprehensive longitudinal analysis of cortical hemispheric structural asymmetries in macaque monkeys at seven age groups at 1, 4, 7, 10, 13, 16, and 19 months of age using multiple distinct cortical properties, for example, cortical surface area, cortical thickness, sulcal depth, and vertex position.

2 | MATERIALS AND METHODS

2.1 | Subjects

This study was performed based on a public rhesus macaque neurodevelopment dataset with 32 macaques (*Macaca mulatta*, 18 males; https://www.nitrc.org/projects/uncuw_macdevmri) (Young et al., 2007). These macaques were reared and housed at the Harlow Primate Laboratory (HPL) at the University of Wisconsin-Madison. Complete rearing, health histories, and pedigrees are known for all animals. Each adult was mated with single sire to ensure that the required number of subjects was met. Only healthy infants were assigned to this study. The older juveniles were housed in small social groups or as a pair to provide companionship after weaning, instead of being reared by their mothers during breast-fed stage, in order to facilitate their normal socialization and ensure standardized rearing conditions. More information on subjects can be found in Young et al. (2007).

2.2 | Image acquisition

Macaques were scanned by using a GE MR750 3.0 T scanner (General Electric Medical, Milwaukee, WI) with the human 8-channel brain array coil at the Waisman Laboratory for Brain Imaging and Behavior at the University of Wisconsin-Madison (Young et al., 2007). T1-weighted images were acquired using an axial inversion recovery (IR) prepared fast gradient echo (fGRE) sequence (GE BRAVO), with parameters: TI/TR/TE = 450/8.684/3.652 ms, FOV = 140 × 140 mm, flip angle = 12°, acquisition matrix = 256 × 256, and voxel size = 0.55 × 0.55 × 0.8 mm^3. T2-weighted images were acquired using a sagittal 3D CUBE FSE sequence, with parameters: TR/TE = 2500/87 ms, FOV = 154 × 154 mm, flip angle = 90°, acquisition matrix = 256 × 256, and voxel size = 0.6 × 0.6 × 0.6 mm^3. Each monkey has 4–5 longitudinal brain MRI scans with the interval of 3–4 months from birth to 20 months old. To characterize the longitudinal development of hemispheric asymmetries, we divided all 134 scans into seven age groups with balanced subject numbers, that is, 1 month (birth−−2 months), 4 months (3–5 months), 7 months (6–8 months), 10 months (9–11 months), 13 months (12–14 months), 16 months (15–17 months), and 19 months (18–20 months) of age. In this way, we also ensured that no two scans from the same monkey was included in the same age group. The number of scans and gender information at each age group are shown in Table 1.

TABLE 1 Number of scans and gender information at each age group

Age group (months)	1 (0–2)	4 (3–5)	7 (6–8)	10 (9–11)	13 (12–14)	16 (15–17)	19 (18–20)
All (32 subjects)	12	21	24	20	22	15	20
Female (14 subjects)	4	8	10	8	8	7	9
Male (18 subjects)	8	13	14	12	14	8	11

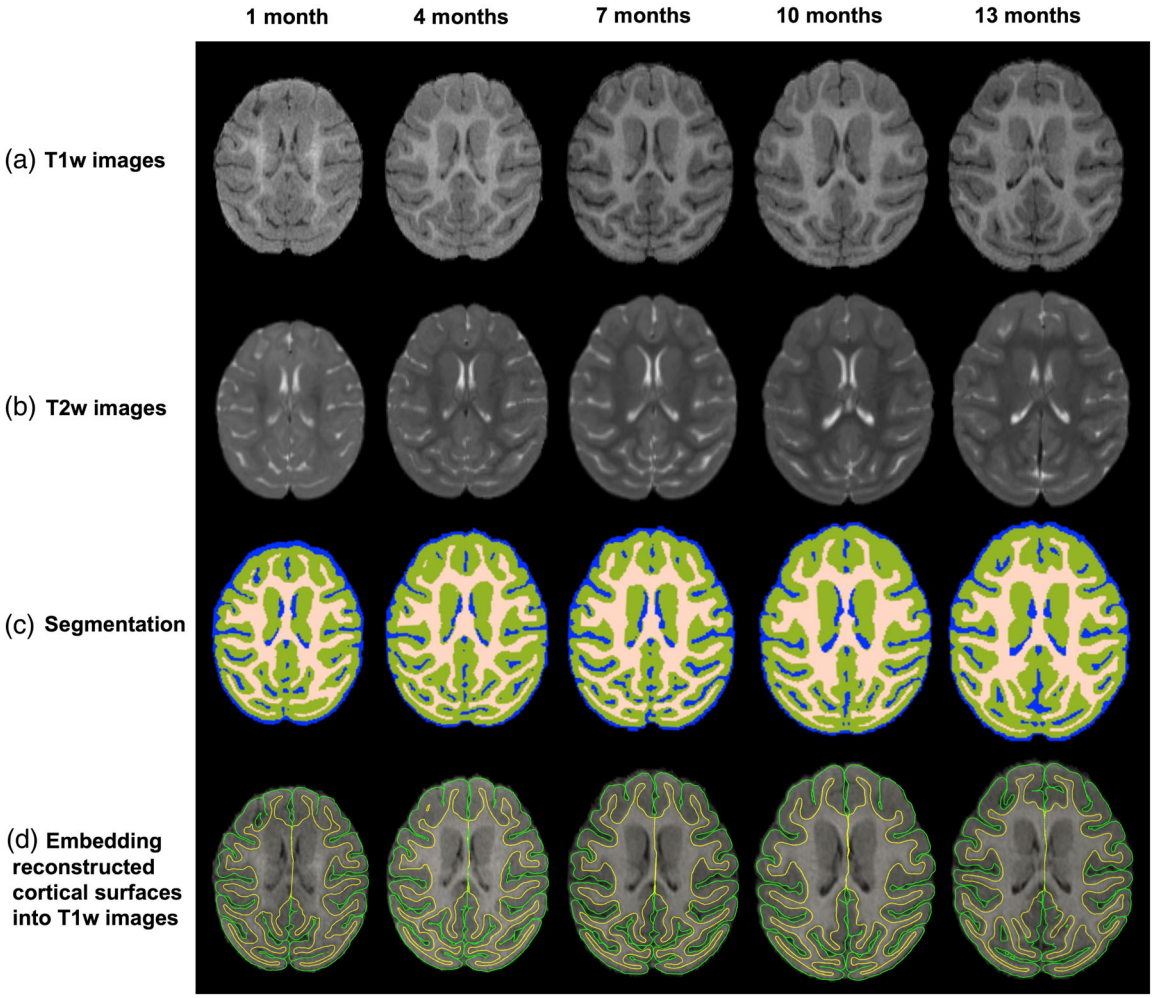

FIGURE 1 The segmentation results of a typical subject with five longitudinal scans from 1 month to 13 months. (a) T1w images; (b) T2w images; (c) Tissue segmentation results; (d) Embedding reconstructed cortical surfaces into T1w images. The yellow curves indicate inner surfaces, and the green curves indicate outer surfaces

2.3 | Image processing and cortical surface mapping

To process longitudinal brain MR images, we followed an infant-specific computational pipeline for cortical surface-based analysis (Wang et al., 2018). First, we rigidly aligned all T2-weighted images onto their corresponding T1-weighted images, and resampled all images to be isotropic with the resolution of $0.55 \times 0.55 \times 0.55$ mm^3. Then, we removed skull, brain stem, and cerebellum. To handle the issue of low tissue contrast appeared in MR images of early postnatal stages, we applied an infant-dedicated learning-based method, coupled with longitudinal guidance (Wang et al., 2013, 2014, 2015), to segment the macaque images into different brain tissues, that is, white matter (WM), gray matter (GM), and cerebrospinal fluid (CSF). We showed the T1w, T2w, and tissue-segmented images from one representative subject with five longitudinal scans from 1 to 13 months in Figure 1. Next, we masked and filled noncortical structures, and separated the left and right hemispheres.

After the above-mentioned steps, for each hemisphere, we corrected topological errors on the inner cortical surface (i.e., white matter surface) using a learning-based method (Sun et al., 2018). Then, we reconstructed inner, central, and outer cortical surfaces by using a topology-preserving deformable surface method (Li, Nie, Wu, et al., 2012; Li et al., 2014; Nie et al., 2011). At each vertex on the reconstructed cortical surfaces, we computed multiple cortical

morphological features, for example, cortical thickness and sulcal depth. Specifically, the cortical thickness of each vertex was computed as the minimum distance between the inner and outer surfaces (Li, Lin, Gilmore, & Shen, 2015). The sulcal depth of each vertex was defined as its distance to the nearest corresponding vertex on the cerebral hull surface, which is a surface running along the margins of gyri without dipping into sulci (Li et al., 2013; Van Essen, 2005). Since the central surface provided a more balanced representation of gyral and sulcal regions (Hill, Dierker, et al., 2010; Li et al., 2013; Van Essen, 2005), we computed the sulcal depth on the central surface in this study. Finally, in order to perform asymmetry analysis between left and right hemispheres, we mirror-flipped the cortical surfaces of right hemisphere to the corresponding left hemisphere along the midsagittal plane, as in human hemispheric asymmetry studies (Li et al., 2013). Next, to perform spherical cortical surface registration, we mapped all cortical surfaces of the left and mirror-flipped right hemispheres onto a spherical space (Fischl, Sereno, & Dale, 1999).

To study longitudinal hemispheric asymmetries, we need to establish both longitudinal (intrasubject) and cross-sectional (intersubject) vertex-to-vertex cortical correspondences. We first established longitudinal cortical correspondences for each subject by unbiased group-wise registration of all longitudinal spherical surfaces, including both the left and mirror-flipped right hemispheres, and then accordingly generated the intrasubject mean cortical folding map using spherical demons (Yeo et al., 2010), as in (Li, Wang, et al., 2015; Wang et al., 2018). For establishing cross-sectional cortical correspondences, we further group-wisely aligned the intrasubject mean cortical folding maps of all subjects and then generated the group-mean cortical folding maps accordingly. Next, based on the two-step registration results, at each age, we resampled the left and mirror-flipped right cortical surfaces along with their cortical thickness and sulcal depth maps of each subject to a standard-mesh tessellation with 163,842 vertices, thus establishing both inter- and intrasubject left–right vertex-to-vertex cortical correspondences across all subjects and ages (Li, Wang, et al., 2015). Finally, for each vertex on each surface, we also computed its surface area based on the resampled central surface (Li, Lin, et al., 2015; Li, Wang, et al., 2015). Herein, the vertex-wise surface area was computed as one-third the sum of the areas of all triangles associated with this vertex (Li, Nie, Wu, et al., 2012). For each vertex in the resampled cortical surface, its vertex position is represented by its 3D coordinate, for studying positional asymmetries between right and left hemispheres. For each vertex, its asymmetry index (AI) of each cortical property (e.g., cortical thickness, surface area, and sulcal depth) was computed as $AI = (\text{left} - \text{right})/[0.5(\text{left} + \text{right})]$ (Li, Lin, et al., 2015). Herein, a positive AI indicates leftward hemispheric asymmetry (with the left side thicker/larger/deeper than the right side), and a negative AI indicates rightward hemispheric asymmetry.

2.4 | Testing significance of hemispheric asymmetries

In each age group, to identify the vertex-wise hemispheric asymmetries of the surface area, cortical thickness, sulcal depth, and the three-dimensional (3D) vertex positions, for each feature, left and right hemispheres were paired and statistically compared. Here, we adopted SurfStat (Chung, Worsley, Nacewicz, Dalton, & Davidson, 2010), a toolbox developed for statistical analysis of cortical surface data based on random field theory (Worsley et al., 2009), which has been used for the mapping of hemispheric structural asymmetries of human brains (Li et al., 2013; Lyttelton et al., 2009). Multiple comparisons were corrected by a random field theory-based cluster analysis (Worsley et al., 2004), using $p < .05$ (two-tailed) cluster-significance threshold.

3 | RESULTS

3.1 | Surface area asymmetries during early brain development

Figure 2a–c shows cortical surface area asymmetries between the left and right hemispheres at 1, 4, 7, 10, 13, 16, and 19 months of age for both lateral and medial views. All results are shown on the age-matched average central cortical surfaces of left hemispheres. On both lateral and medial surfaces, the overall patterns of left-larger-than-right (red color) and right-larger-than-left (blue color) are relatively consistent across all age groups. Leftward asymmetries are most prominent in the temporal and occipital cortices, while rightward asymmetries are most prominent in the frontal and parietal cortices. Figure 2a shows the AI values of surface area, Figure 2b shows the *t*-statistic maps, and Figure 2c shows clusters that pass significance testing ($p < .05$) after correction for multiple comparisons. Table 2 provides the average AI values of surface area for the 10 major clusters of asymmetries in Figure 2c in all subjects at 1, 4, 7, 10, 13, 16, and 19 months of age.

The clusters of leftward and rightward asymmetries expand remarkably from 1 to 4 months, and then keep relatively stable. Specifically, on the lateral surface, several significant clusters of asymmetries are consistently identified from 1 to 19 months, including leftward asymmetries in the ventral occipital cortex, anterior IFG, posterior insula, posterior middle STS, as well as rightward asymmetries in the dorsal precentral gyrus, anterior middle STS, anterior occipital cortex, and angular gyrus. From 1 to 19 months, the clusters of rightward asymmetries in the anterior middle STS, anterior occipital cortex, and angular gyrus gradually expand to include larger areas. Two portions in the middle and posterior superior temporal gyrus (STG) show no asymmetry at 1 month, but with leftward asymmetries from 4 to 19 months. Two clusters at the inferior and superior postcentral gyri show rightward asymmetries from 1 month to 16 months, but disappear at 19 months. A small region in the inferior precentral gyrus shows rightward asymmetry from 4 months, and gradually enlarges to include larger areas and parts of the inferior arcuate sulcus and IFG from 7 to 19 months.

On the medial surface, several significant clusters are consistently identified from 1 to 19 months, including the rightward asymmetries around the cingulate cortex, temporal pole, and a portion in the medial occipital cortex. A portion in the precuneus cortex shows leftward asymmetry at 1 month, but gradually shrinks and then disappears at 7 months.

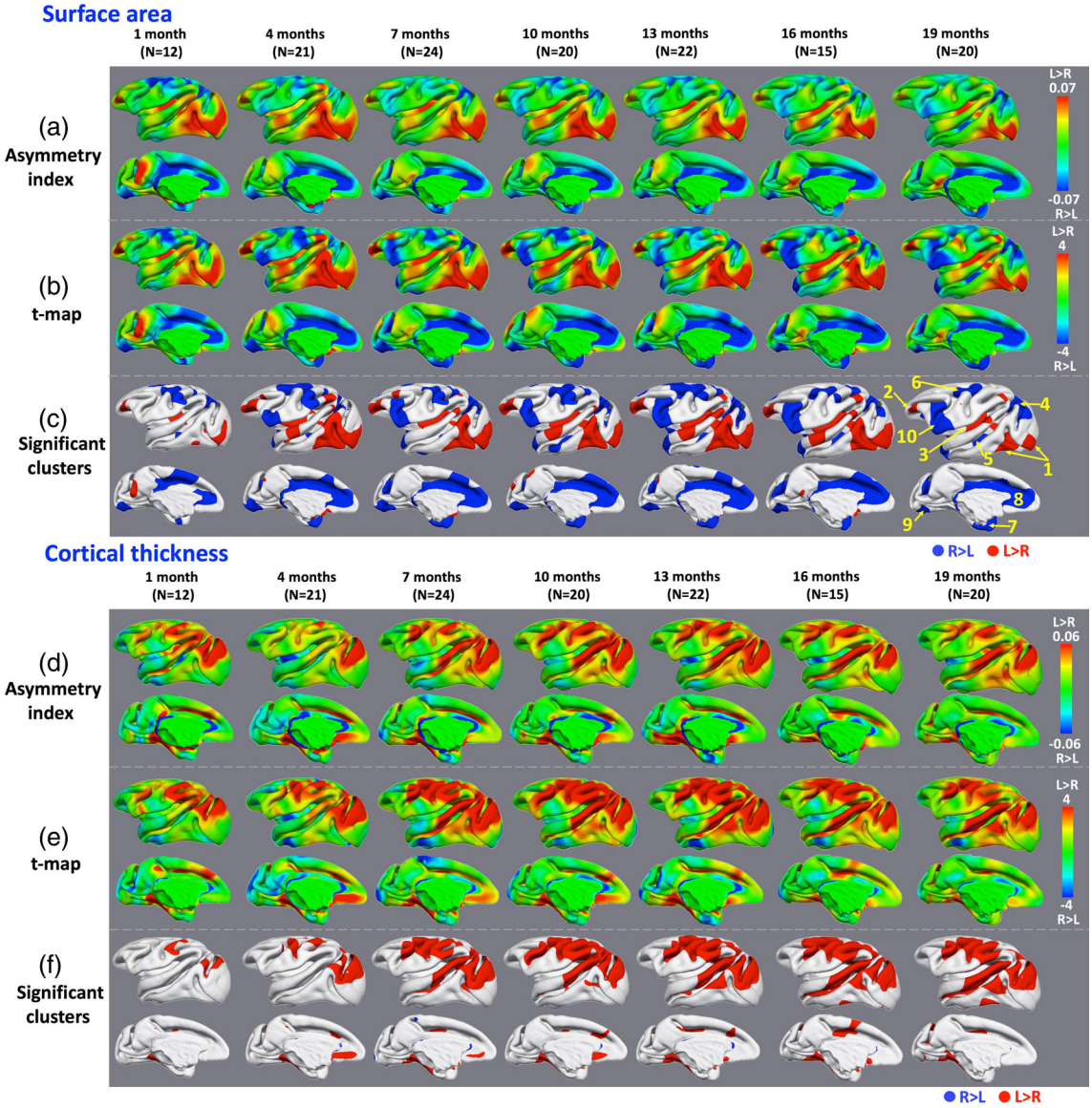

FIGURE 2 Hemispheric asymmetries of surface area and cortical thickness. (a) and (d): asymmetry index (AI) maps of surface area and cortical thickness, respectively. (b) and (e): Paired t-maps of left–right values of the surface area and cortical thickness, respectively. (c) and (f): Significant clusters of hemispheric asymmetries of surface area ($p < .05$) and cortical thickness ($p < .05$) after correction for multiple comparisons, respectively. Blue clusters indicate rightward asymmetries and red clusters indicate leftward asymmetries

3.2 | Cortical thickness asymmetries during early brain development

The cortical thickness asymmetries between left and right hemispheres at 1, 4, 7, 10, 13, 16, and 19 months of age for both lateral and medial views are shown in Figure 2d–f. All results are shown on the age-matched average central cortical surfaces of left hemispheres. On both lateral and medial surfaces, unlike surface area, most regions present left-thicker-than-right (red color) asymmetries, especially prominent in the dorsal frontal cortex, parietal cortex, anterior occipital cortex and superior temporal cortex. Figure 2d shows the AI values of cortical thickness, Figure 2e shows the *t*-statistic maps, and Figure 2f shows clusters that pass significance testing ($p < .05$) after correction for multiple comparisons.

Overall, the clusters of leftward asymmetries enlarge remarkably from 1 to 7 months, and then keep relatively stable until to 19 months. Specifically, on the lateral surface, several significant clusters of asymmetries are consistently identified, including the postcentral gyrus, anterior occipital cortex, and posterior STG. The clusters of leftward asymmetries in the postcentral gyrus and anterior occipital cortex are relatively small at 1 month, and gradually expand from 4 to 19 months. A large portion in the STG exhibits leftward asymmetry at 7 months, and gradually expands to include the PT from 10 to 19 months. A small portion in the precentral gyrus exhibits leftward asymmetry at 4 months and gradually expands to include the arcuate sulcus from 7 to 19 months. An anterior portion in the STS shows leftward asymmetry from 7 to 19 months.

On the medial surface, two significant clusters of leftward asymmetries are consistently identified from 1 to 19 months, including the medial temporal cortex and posterior cingulate sulcus. A portion in

TABLE 2 The asymmetry index (AI) values of surface area of major significant clusters from 1 to 19 months

Significant clusters	1 month	4 months	7 months	10 months	13 months	16 months	19 months
(1) Ventral occipital cortex	0.089	0.071	0.061	0.065	0.063	0.062	0.059
(2) Inferior frontal gyrus	0.054	0.045	0.042	0.042	0.042	0.044	0.036
(3) Posterior insula and posterior superior temporal gyrus	0.080	0.045	0.052	0.053	0.050	0.062	0.053
(4) Anterior occipital cortex and angular gyrus	−0.051	−0.034	−0.051	−0.045	−0.047	−0.047	−0.055
(5) Anterior middle superior temporal sulcus	−0.058	−0.047	−0.048	−0.042	−0.042	−0.052	−0.050
(6) Dorsal precentral gyrus	−0.068	−0.075	−0.035	−0.044	−0.043	−0.056	−0.036
(7) Temporal pole	−0.082	−0.061	−0.051	−0.057	−0.057	−0.048	−0.061
(8) Cingulate cortex	−0.086	−0.075	−0.076	−0.086	−0.090	−0.085	−0.071
(9) Inferior occipital gyrus	−0.059	−0.048	−0.052	−0.045	−0.056	−0.048	−0.045
(10) Inferior precentral gyrus	-	−0.034	−0.033	−0.037	−0.032	−0.039	−0.040

the medial orbitofrontal cortex shows leftward asymmetry at 4 months, yet gradually shrinks and finally disappears at 19 months.

3.3 | Sulcal depth asymmetries during early brain development

The sulcal depth asymmetries between left and right hemispheres at 1, 4, 7, 10, 13, 16, and 19 months of age for both lateral and medial views are shown in Figure 3a–c. To inspect deep sulcal regions more clearly, all results are shown on the age-matched average inner cortical surfaces of left hemispheres. On both lateral and medial surfaces, the patterns of left-deeper-than-right (red color) and right-deeper-than-left (blue color) are largely consistent from 4 to 19 months. Left-deeper-than-right asymmetries are most prominent in the principal sulcus and inferior temporal gyrus, while rightward asymmetries are most prominent in the inferior precentral gyrus, insula, STS, and cingulate cortex. Figure 3a shows the AI values of sulcal depth, Figure 3b shows the *t*-statistic maps, and Figure 3c shows clusters that pass significance testing ($p < .05$) after correction for multiple comparisons. Table 3 provides the average AI values of sulcal depth for the major clusters of asymmetries at different age groups.

Most clusters of rightward and leftward asymmetries appear at 4 months, except the cluster of rightward asymmetries at the anterior cingulate cortex (ACC) that appears at 1 month. The clusters of rightward asymmetries expand remarkably from 4 to 7 months, and then keep relatively stable until to 19 months. Oppositely, the clusters of leftward asymmetries shrink remarkably from 4 to 7 months, and finally disappear at 19 months. Specifically, on the lateral surface, there is no significant cluster at 1 month. Several significant clusters of asymmetries are consistently identified from 4 to 19 months, including right-deeper-than-left asymmetries in the anterior and posterior insula, anterior and posterior STS, and inferior precentral gyrus. The clusters of left-deeper-than-right in the principal sulcus and posterior inferior temporal gyrus gradually shrink from 4 to 16 months, and finally disappear at 19 months. The cluster of right-deeper-than-left asymmetry in the inferior precentral gyrus gradually expands from 4 to 13 months, and remains stable from 16 to 19 months. The clusters of right-deeper-than-left asymmetries in the anterior insula and posterior STS gradually expand to include more regions from 4 to 7 months, and remain stable from 10 to 19 months. A large portion at the dorsal arcuate sulcus shows right-deeper-than-left asymmetry from 16 to 19 months. Two small portions at the intraparietal sulcus exhibit right-deeper-than-left asymmetries at 10 and 13 months, and further expand from 16 to 19 months.

On the medial surface, only the right-deeper-than-left asymmetry in ACC is consistently identified from 1 to 19 months. A large portion at the cuneus exhibits right-deeper-than-left asymmetry at 4 months. However, this cluster shrinks to a smaller cluster at 7 months and disappears at 10 months.

3.4 | Cortical vertex position asymmetries during early brain development

Figure 3d–g shows the cortical vertex position asymmetries between left and mirror-flipped right hemispheres at 1, 4, 7, 10, 13, 16, and 19 months of age for both lateral and medial views. Specifically, Figure 3d, e show the average cortical surfaces of left and mirror-flipped right hemispheres, respectively, color-coded by the magnitude of the deformation between their respective average cortical surfaces. The average cortical surface of each hemisphere at each age was generated by averaging the 3D positions of corresponding vertices of all middle cortical surfaces of the hemisphere. The major cortical folding patterns are strikingly similar between left and right hemispheres. Figure 3f shows clusters that pass significance testing of 3D vertex position asymmetry ($p < .05$) after correction for multiple comparisons. The arrows in Figure 3f indicate the deformation field from the average cortical surface of the left hemisphere to the average cortical surface of the mirror-flipped right hemisphere.

Overall, the asymmetric clusters expand remarkably from 1 to 4 months, and then keep relatively stable thereafter. Specifically, on the lateral surface, the STG is consistently identified as a region with significant asymmetries at all ages from 1 to 19 months. As shown in the enlarged cropped regions of the anterior STG in Figure 3g, the clusters at the left anterior and posterior STG are found to be located more

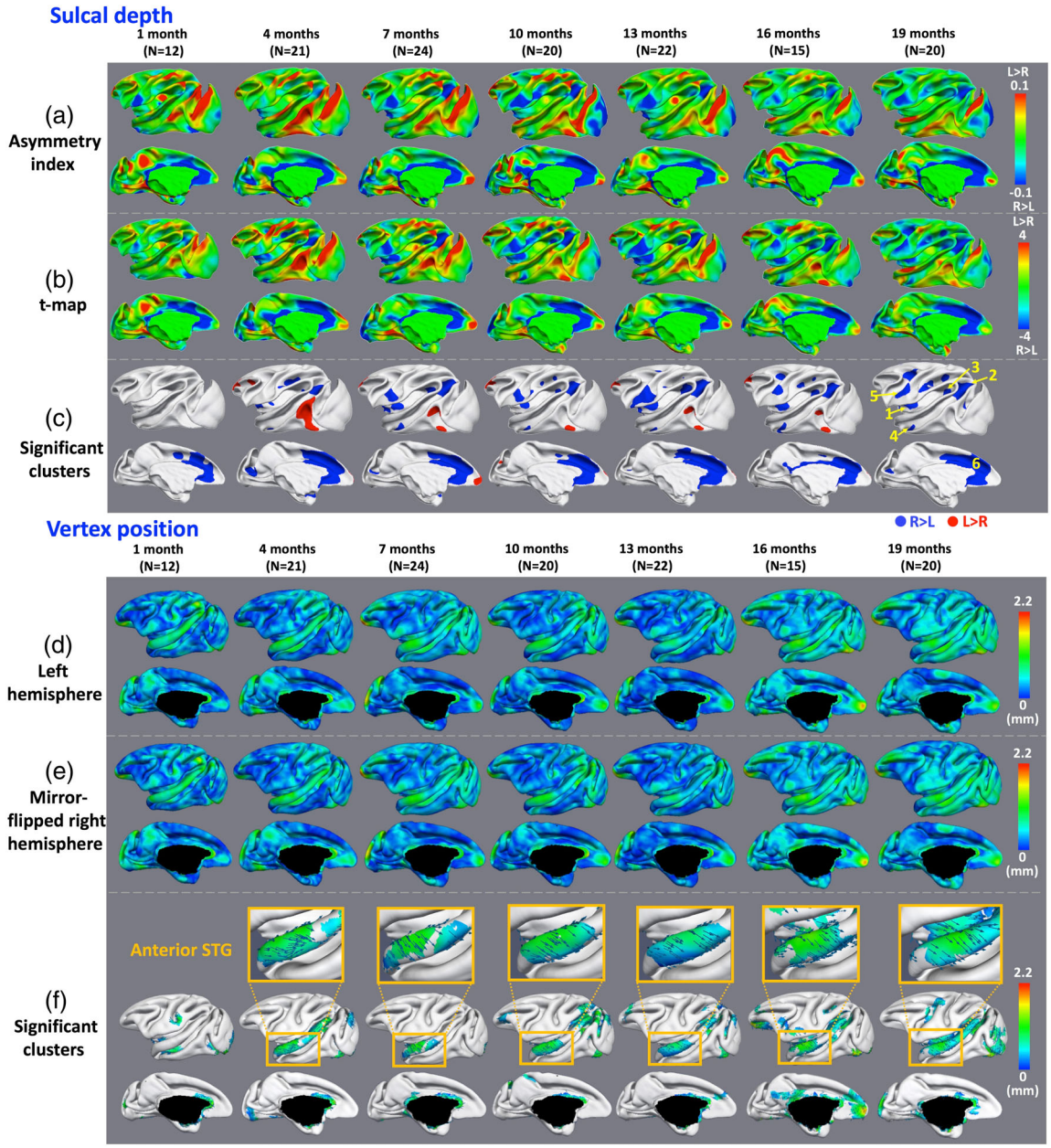

FIGURE 3 Hemispheric asymmetries of sulcal depth and vertex position of the cortex. (a) Maps of asymmetry index (AI) of sulcal depth. (b) Paired t-maps of left–right values of sulcal depth. (c) Significant clusters of hemispheric asymmetries of sulcal depth ($p < .05$) after correction for multiple comparisons. Blue clusters indicate rightward asymmetries and red clusters indicate leftward asymmetries. (d) and (e) Magnitude maps of the deformation from the left hemispheres to the mirror-flipped right hemispheres, shown on the age-matched, left and mirror-flipped right average central surfaces, respectively. (f) Significant clusters of hemispheric asymmetries of 3D vertex positions between left and mirror-flipped right hemispheres ($p < .05$) after correction for multiple comparisons, and the 3D deformation vectors from left to mirror-flipped right cortical surfaces

TABLE 3 The asymmetry index (AI) values of sulcal depth of major significant clusters from 1 to 19 months

Significant clusters	1 month	4 months	7 months	10 months	13 months	16 months	19 months
(1) Anterior insula	-	−0.084	−0.565	−0.036	−0.064	−0.029	−0.023
(2) Posterior superior temporal sulcus	-	−0.043	−0.077	−0.060	−0.068	−0.069	−0.072
(3) Posterior insula	-	−0.029	−0.172	−0.024	−0.046	−0.043	−0.047
(4) Anterior superior temporal sulcus	-	−0.043	−0.043	−0.045	−0.039	−0.092	−0.050
(5) Inferior precentral gyrus	-	−0.067	−0.089	−0.077	−0.080	−0.051	−0.054
(6) Anterior cingulate cortex	−0.226	−0.197	−0.041	−0.195	−0.163	−0.204	−0.161

anterior, compared to the right ones from 4 to 19 months. A region in the left ventral occipital cortex is also found to be located more anterior, when compared to the right ventral occipital cortex at 4 months. This asymmetry disappears at 7 months, but reappears at 10 months and gradually expands from 16 to 19 months. On the medial surface, prominent asymmetries are observed around the ACC from 16 and 19 months. The cluster in the left ACC is found to be located more posterior, compared to the right one from 4 to 19 months.

4 | DISCUSSION

For the first time, we comprehensively analyzed the hemispheric structural asymmetries of healthy macaque monkeys from birth to 19 months using cortical surface-based morphometry. Overall, most asymmetric clusters on the surface area, cortical thickness, sulcal depth, and vertex positions are present in the first 4 months and are relatively consistent from 4 to 19 months. Importantly, each cortical property exhibits distinct asymmetric patterns, evolving with the age. Specifically, the clusters of leftward and rightward asymmetries of surface area expand remarkably from 1 to 4 months, and then keep relatively stable. Cortical thickness only exhibits leftward asymmetries, and the clusters expand remarkably from 1 to 7 months and then keep relatively stable until to 19 months. Most clusters of leftward and rightward asymmetries of sulcal depth appear at 4 months, dissimilar with studies in human that many cortical hemispheric asymmetries of sulcal depth arise in the later fetal stage (Habas et al., 2011; Li et al., 2013) and are present obviously at birth. Moreover, in our results, the clusters of rightward asymmetries of sulcal depth expand remarkably from 4 to 7 months, and remain stable until 19 months, while the clusters of leftward asymmetries of sulcal depth shrink considerably from 4 to 16 months and finally disappear at 19 months. The asymmetric clusters of vertex position expand remarkably from 1 to 4 months, and then keep relatively stable.

For the cortical surface area, leftward asymmetries are consistently found around the STG, IFG, and posterior insula, whereas rightward asymmetries are consistently found around the middle STS and temporal pole from 1 to 19 months, largely consistent with the studies in both adult nonhuman primates (e.g., macaque monkeys, baboons, and chimpanzees) and human. In nonhuman studies, a similar rightward asymmetry of surface area at STS has been found in adult macaque monkeys (Bogart et al., 2012); however, this rightward asymmetry is scarce in studies of baboons and chimpanzees. Similar leftward asymmetries of surface area at the PT, which is located at the posterior STG, and the Broca's area, which is located at the posterior IFG, are reported in adult baboons (Cantalupo & Hopkins, 2001; Marie et al., 2017) and adult chimpanzees (Bogart et al., 2012; Cantalupo & Hopkins, 2001; Hopkins & Nir, 2010; Lyn et al., 2011). In our results, two clusters at the inferior and superior postcentral gyrus show rightward asymmetries from 1 to 16 months, in line with the findings that rightward asymmetry of surface area at the inferior postcentral gyrus in adult chimpanzees (Bogart et al., 2012; Gilissen & Hopkins, 2012). In human infant studies, a similar rightward asymmetry of surface area at the temporal pole has been found in (Li et al., 2013). Moreover, similar leftward asymmetries of surface area at STG and posterior insula, as well as rightward asymmetries of surface area at STS, have been reported from the later fetal stage to adulthood (Dubois et al., 2010; Habas et al., 2011; Li et al., 2013; Van Essen et al., 2011). Our findings thus suggest that leftward asymmetries in the STG and posterior insula and rightward asymmetries in the STS and temporal pole might not be human-specific.

For the cortical thickness, most leftward asymmetries are found in the dorsal frontal cortex, parietal cortex, anterior occipital cortex, and superior temporal cortex. Existing studies on the hemispheric asymmetries of cortical thickness in macaque monkeys are scarce. In a recent study, leftward asymmetries of cortical volume have been found in the frontal and parietal cortices in macaque monkeys from 1 week to 52 months (Scott et al., 2016), which might be associated with their leftward asymmetries of cortical thickness revealed in our results. Our results also show leftward asymmetries at the medial temporal cortex and posterior cingulate cortex from 1 to 19 months, in line with the findings in human infants from birth to 2 years of age (Li, Lin, et al., 2015). In addition, in our results, the leftward asymmetry of cortical thickness shown in the precentral gyrus is largely consistent with the studies in human infants which show thicker cortex at the left precentral gyrus than the right one (Li, Lin, et al., 2015). These results suggest that macaque monkeys also exhibit hemispheric asymmetries of cortical thickness, although their spatiotemporal patterns are different from those of human.

The PT, a cerebral region making up the superior surface of the posterior STG to the parietal lobe (Clark, Boutros, & Mendez, 2007), is considered as one of the functional epicenters of the language network, because it is in part overlapping with Wernicke's area (Mesulam, 1998) and contains auditory association cortex (Galaburda, Sanides, & Geschwind, 1978). Although in previous studies leftward asymmetries of cortical volume and surface area at PT have been found in chimpanzees (Bogart et al., 2012; Hopkins & Nir, 2010), baboons (Kochunov et al., 2010; Lyn et al., 2011; Marie et al., 2017), and human (Li et al., 2013; Lyttelton et al., 2009), these asymmetries have never been reported in neuroimaging studies of macaque monkeys. For the first time, we revealed left-thicker-than-right asymmetries at PT in macaque monkeys from 1 to 19 months, thus confirming the findings at the cellular level, which reported a leftward volumetric asymmetry in the cytoarchitecture at PT in macaque monkeys (Gannon et al., 2008). However, having leftward PT asymmetries of cortical thickness does not make the macaque monkeys to have a language-ready brain, despite their intentional gestural communicatory system (Fitch, de Boer, Mathur, & Ghazanfar, 2016). In fact, the hypothesis of a lack of neural circuitry enabling language and sophisticated vocal control in monkeys has recently been highlighted (Fitch et al., 2016), showing that anatomical constraints of the vocal apparatus might not be enough to support monkeys to produce vowels.

For the sulcal depth, the cluster of left-deeper-than-right asymmetry is found at the posterior inferior temporal gyrus from 1 to 16 months, similar to the findings in adult chimpanzees (Bogart et al.,

2012). For the first time, we find the cluster of right-deeper-than-left at the posterior insula cortex gradually expands from 4 to 7 months and remains stable from 10 to 19 months. This result is in line with that in human infant studies, which have reported right-deeper-than-left asymmetries at the posterior insula at birth, 1 year, and 2 years of age (Li et al., 2013). Moreover, the cluster of right-deeper-than-left in the STS expands substantially from 4 to 7 months, and remains stable from 10 to 19 months, generally consistent with the studies in human fetuses (Habas et al., 2011), infants (Li et al., 2013), and adults (Hill, Dierker, et al., 2010), which have reported the right-deeper-than-left asymmetry in the STS.

The prominent asymmetries of cortical vertex positions in macaque monkeys are consistently observed around the STG and anterior occipital cortex, with the left STG being more anterior to the right STG. However, these findings are dissimilar with the findings in human infants (Glasel et al., 2011; Li et al., 2013) and adults (Van Essen et al., 2011), in which the left STG is found to be located more posterior, compared to the right one. In our results, the magnitudes of the asymmetries increase from 1 to 19 months of age, due to the remarkable brain development, which are similar with the findings in human infants from 0 to 2 years of age (Li et al., 2013).

In our results, the asymmetric clusters of the surface area and cortical thickness show totally different patterns at all-time points from 1 to 19 months, which are largely consistent with the findings in human infants (Li et al., 2013; Li, Lin, et al., 2015). Specifically, the asymmetric clusters of the surface area appear around the prefrontal, anterior temporal, posterior occipital, and cingulate cortices, while the asymmetric clusters of the cortical thickness appear around the postcentral gyrus, posterior temporal, parietal and anterior occipital cortices. Although both the surface area and cortical thickness show asymmetries around the central sulcus, the surface area exhibits rightward asymmetries, while the cortical thickness shows leftward asymmetries. Many studies have indicated that cortical thickness and surface area have distinct genetic underpinnings and cellular mechanisms (Panizzon et al., 2009). Meanwhile, several studies further suggested that perinatal environment has different influences on the development of surface area and cortical thickness (Lyall et al., 2014). Therefore, the distinct genetic underpinnings, cellular mechanisms, and environmental factors might jointly contribute to the differential developmental patterns of surface area and cortical thickness during infancy, thus leading to the different hemispheric asymmetries of these two distinct features in our study.

The asymmetries in the sulcal depth reflect uneven deepening of sulci on the left and right hemispheres (Bogart et al., 2012). It has shown three overlapped clusters with the asymmetries in surface area, including the rightward asymmetries at the inferior precentral gyrus (Cluster 10 in surface area and Cluster 5 in sulcal depth), anterior STS (Cluster 5 in surface area and Cluster 4 in sulcal depth) and ACC (Cluster 8 in surface area and Cluster 6 in sulcal depth). One reason for these similar hemispheric asymmetric clusters of the sulcal depth and surface area is that the uneven deepening of sulci is usually accompanied by uneven expansion of surface area. However, as uneven widening or lengthening of sulci or gyri would also result in the expansion of surface area (Xia, Wang, et al., 2018), there are still many different asymmetric clusters between these two features. The hemispheric asymmetries of vertex positions can provide important information on cortical shape asymmetries between right and left hemispheres. Different from those of other three measures, the asymmetric clusters of vertex position are mainly located around the anterior STG.

5 | LIMITATIONS

Although our studies systemically provided the normal cortical hemispheric structural asymmetries from 1 to 19 months of age using surface area, cortical thickness, sulcal depth, and vertex position, there still are some limitations to state. First, the large intersubject variability among monkeys in different age groups might influence our asymmetries results. Due to the accelerated longitudinal design of this study, each subject was scanned 4–5 times with different starting age, making the numbers of subjects at different time points unbalanced, and the 1-month-group has the least number of subjects. We also noted that the cortices of macaque monkeys develop more rapidly during the first few months of life (Malkova et al., 2006; Scott et al., 2016). These factors might lead to larger intersubject variability among monkeys in the 1-month-group, compared to those in later months, which might have some influences on the estimated hemispheric asymmetries. To investigate these influences, we have also controlled the sample size across the first two age groups, and compared the updated results with our original results, and added these results in Table S1, Figure S1, and Figure S2. We found that the overall changing patterns of asymmetric regions remain largely similar, although there exist slight changes related to subject numbers. Second, during the early stage of life in both humans and macaques, the subcortical structures also develop rapidly and play critical roles in brain functions and behaviors, as the majority of cortical structures are immature (Gilmore et al., 2011; Scott et al., 2016). Specifically, in the human brain, the total volume of subcortical structures increases at a rate between 104 and 107% in the first postnatal year (Gilmore et al., 2011). In the macaque brain, the total volume of subcortical structures also increases rapidly during the first year of life (Scott et al., 2016). Moreover, the development of subcortical structures in macaque monkeys is closely related to the formation and maturation of motor and auditory functions (Bruni et al., 2018; Scott et al., 2016). Therefore, it is also of great importance to study the development and asymmetries of subcortical structures during infancy in our future work.

6 | CONCLUSION

By leveraging an infant-dedicated pipeline for cortical surface-based morphometry, we have systemically characterized the normal cortical hemispheric structural asymmetries at 1, 4, 7, 10, 13, 16, and 19 months of age using multiple distinct cortical properties, for example, cortical surface area, cortical thickness, sulcal depth, and vertex position, in macaque monkeys. This is the first comprehensive study of longitudinal developmental trajectories of cortical hemispheric asymmetries in the

early stage of life of macaque monkeys. Our findings suggest that the leftward areal asymmetries of the STG and IFG, leftward thickness asymmetries of the medial temporal cortex, precentral, and posterior cingulate cortex, and also the rightward depth asymmetries of the STS are not human-specific, since they are all present in our macaque studies. Our study provides important new insights into early brain development and evolution, although the biological mechanisms of our identified hemispheric asymmetries are still unclear.

ACKNOWLEDGMENTS

G. Li was supported in part by NIH grants (MH107815, MH116225, and MH117943). L. Wang was supported in part by NIH grants (MH109773 and MH117943). D. Shen was supported in part by NIH grant (MH117943). Thank Dr. Martin A. Styner and his colleagues for making the UNC-Wisconsin neurodevelopment rhesus MRI database publicly available.

DATA AVAILABILITY STATEMENT

The data that support the findings of this study are openly available in NITRC at https://www.nitrc.org/projects/uncuw_macdevmri.

ORCID

Jing Xia https://orcid.org/0000-0003-4962-2604
Li Wang https://orcid.org/0000-0003-2165-0080

REFERENCES

Bauman, M., Iosif, A., Ashwood, P., Braunschweig, D., Lee, A., Schumann, C., … Amaral, D. (2013). Maternal antibodies from mothers of children with autism alter brain growth and social behavior development in the rhesus monkey. *Translational Psychiatry*, *3*(7), e278.

Benkarim, O. M., Sanroma, G., Zimmer, V. A., Muñoz Moreno, E., Hahner, N., Eixarch, E., … Piella, G. (2017). Toward the automatic quantification of in utero braindevelopment in 3D structural MRI: A review. *Humanbrain mapping*, *38*(5), 2772–2787.

Bogart, S. L., Mangin, J.-F., Schapiro, S. J., Reamer, L., Bennett, A. J., Pierre, P. J., & Hopkins, W. D. (2012). Cortical sulci asymmetries in chimpanzees and macaques: A new look at an old idea. *NeuroImage*, *61*(3), 533–541.

Bruni, S., Gerbella, M., Bonini, L., Borra, E., Coudé, G., Ferrari, P. F., … Function. (2018). Cortical and subcortical connections of parietal and premotor nodes of the monkey hand mirror neuron network. *Brain Structure & Function*, *223*(4), 1713–1729.

Cantalupo, C., & Hopkins, W. D. (2001). Asymmetric Broca's area in great apes. *Nature*, *414*(6863), 505.

Chen, Y., Yu, J., Niu, Y., Qin, D., Liu, H., Li, G., … Kang, Y. (2017). Modeling Rett syndrome using TALEN-edited MECP2 mutant cynomolgus monkeys. *Cell*, *169*(5), 945–955 e910.

Chung, M. K., Worsley, K. J., Nacewicz, B. M., Dalton, K. M., & Davidson, R. J. (2010). General multivariate linear modeling of surface shapes using SurfStat. *NeuroImage*, *53*(2), 491–505.

Clark, D. L., Boutros, N. N., & Mendez, M. F. (2007). The brain and behavior: An introduction to behavioral neuroanatomy. Cambridge university press, 2010.

Clouchoux, C., Kudelski, D., Gholipour, A., Warfield, S. K., Viseur, S., Bouyssi-Kobar, M. … Limperopoulos, C. (2012). Quantitative in vivo MRI measurement ofcortical development in the fetus. *BrainStructure and Function*, *217*(1), 127–139.

Davatzikos, C., & Bryan, R. N. (2002). Morphometric analysis of cortical sulci using parametric ribbons: A study of the central sulcus. *Journal of Computer Assisted Tomography*, *26*(2), 298–307.

Dubois, J., Benders, M., Cachia, A., Lazeyras, F., Ha-Vinh Leuchter, R., Sizonenko, S., … Hüppi, P. S. (2007). Mapping the early cortical folding process in thepreterm newborn brain. *Cerebral Cortex*, *18*(6), 1444–1454.

Dubois, J., Benders, M., Lazeyras, F., Borradori-Tolsa, C., Leuchter, R. H.-V., Mangin, J.-F., & Hüppi, P. S. (2010). Structural asymmetries of perisylvian regions in the preterm newborn. *NeuroImage*, *52*(1), 32–42.

Dubois, J., & Dehaene-Lambertz, G. (2015). Fetal and postnatal development of thecortex: MRI and genetics. In Toga AW (Ed.), *Brain Mapping: An Encyclopedic Reference* (pp. 11–19). Waltham, MA: Academic Press (Elsevier).

Fischl, B., Sereno, M. I., & Dale, A. M. (1999). Cortical surface-based analysis: II: Inflation, flattening, and a surface-based coordinate system. *NeuroImage*, *9*(2), 195–207.

Fitch, W. T., de Boer, B., Mathur, N., & Ghazanfar, A. A. (2016). Monkey vocal tracts are speech-ready. *Science Advances*, *2*(12), e1600723.

Galaburda, A. M., Sanides, F., & Geschwind, N. (1978). Human brain: Cytoarchitectonic left-right asymmetries in the temporal speech region. *Archives of Neurology*, *35*(12), 812–817.

Gannon, P. J., Holloway, R. L., Broadfield, D. C., & Braun, A. R. (1998). Asymmetry of chimpanzee planum temporale: Humanlike pattern of Wernicke's brain language area homolog. *Science*, *279*(5348), 220–222.

Gannon, P. J., Kheck, N., & Hof, P. R. (2008). Leftward interhemispheric asymmetry of macaque monkey temporal lobe language area homolog is evident at the cytoarchitectural, but not gross anatomic level. *Brain Research*, *1199*, 62–73.

Gilissen, E. P., & Hopkins, W. D. (2012). Asymmetries of the parietal operculum in chimpanzees (*Pan troglodytes*) in relation to handedness for tool use. *Cerebral Cortex*, *23*(2), 411–422.

Gilmore, J. H., Shi, F., Woolson, S. L., Knickmeyer, R. C., Short, S. J., Lin, W., … Shen, D. (2011). Longitudinal development of cortical and subcortical gray matter from birth to 2 years. *Cerebral Cortex*, *22*(11), 2478–2485. https://doi.org/10.1093/cercor/bhr327%J

Glasel, H., Leroy, F., Dubois, J., Hertz-Pannier, L., Mangin, J.-F., & Dehaene-Lambertz, G. (2011). A robust cerebral asymmetry in the infant brain: The rightward superior temporal sulcus. *NeuroImage*, *58*(3), 716–723.

Habas, P. A., Scott, J. A., Roosta, A., Rajagopalan, V., Kim, K., Rousseau, F., … Studholme, C. (2011). Early folding patterns and asymmetries of the normal human brain detected from in utero MRI. *Cerebral Cortex*, *22*(1), 13–25.

Hamilton, L. S., Narr, K. L., Luders, E., Szeszko, P. R., Thompson, P. M., Bilder, R. M., & Toga, A. W. (2007). Asymmetries of cortical thickness: Effects of handedness, sex, and schizophrenia. *Neuroreport*, *18*(14), 1427–1431.

Hill, J., Dierker, D., Neil, J., Inder, T., Knutsen, A., Harwell, J., … Van Essen, D. (2010). A surface-based analysis of hemispheric asymmetries and folding of cerebral cortex in term-born human infants. *Journal of Neuroscience*, *30*(6), 2268–2276.

Hill, J., Inder, T., Neil, J., Dierker, D., Harwell, J., & Van Essen, D. (2010). Similar patterns of cortical expansion during human development and evolution. *Proceedings of the National Academy of Sciences*, *107*(29), 13135–13140.

Hopkins, W. D., Marino, L., Rilling, J. K., & MacGregor, L. A. (1998). Planum temporale asymmetries in great apes as revealed by magnetic resonance imaging (MRI). *Neuroreport*, *9*(12), 2913–2918.

Hopkins, W. D., Meguerditchian, A., Coulon, O., Misiura, M., Pope, S., Mareno, M. C., & Schapiro, S. J. (2017). Motor skill for tool-use is

associated with asymmetries in Broca's area and the motor hand area of the precentral gyrus in chimpanzees (*Pan troglodytes*). *Behavioural Brain Research*, *318*, 71–81.

Hopkins, W. D., Misiura, M., Pope, S. M., & Latash, E. M. (2015). Behavioral and brain asymmetries in primates: A preliminary evaluation of two evolutionary hypotheses. *Annals of the New York Academy of Sciences*, *1359*(1), 65–83.

Hopkins, W. D., & Nir, T. M. (2010). Planum temporale surface area and grey matter asymmetries in chimpanzees (*Pan troglodytes*): The effect of handedness and comparison with findings in humans. *Behavioural Brain Research*, *208*(2), 436–443.

Kochunov, P., Glahn, D. C., Fox, P. T., Lancaster, J. L., Saleem, K., Shelledy, W., … Mangin, J.-F. (2010). Genetics of primary cerebral gyrification: Heritability of length, depth and area of primary sulci in an extended pedigree of Papio baboons. *NeuroImage*, *53*(3), 1126–1134.

Lewis, D. A. (1997). Development of the prefrontal cortex during adolescence: Insights into vulnerable neural circuits in schizophrenia. *Neuropsychopharmacology*, *16*(6), 385–398.

Li, G., Lin, W., Gilmore, J. H., & Shen, D. (2015). Spatial patterns, longitudinal development, and hemispheric asymmetries of cortical thickness in infants from birth to 2 years of age. *Journal of Neuroscience*, *35*(24), 9150–9162.

Li, G., Nie, J., Wang, L., Shi, F., Gilmore, J. H., Lin, W., & Shen, D. (2014). Measuring the dynamic longitudinal cortex development in infants by reconstruction of temporally consistent cortical surfaces. *NeuroImage*, *90*, 266–279.

Li, G., Nie, J., Wang, L., Shi, F., Lin, W., Gilmore, J. H., & Shen, D. (2012). Mapping region-specific longitudinal cortical surface expansion from birth to 2 years of age. *Cerebral Cortex*, *23*(11), 2724–2733.

Li, G., Nie, J., Wang, L., Shi, F., Lyall, A. E., Lin, W., … Shen, D. (2013). Mapping longitudinal hemispheric structural asymmetries of the human cerebral cortex from birth to 2 years of age. *Cerebral Cortex*, *24*(5), 1289–1300.

Li, G., Nie, J., Wu, G., Wang, Y., Shen, D., & Initiative, A. S. D. N. (2012). Consistent reconstruction of cortical surfaces from longitudinal brain MR images. *NeuroImage*, *59*(4), 3805–3820.

Li, G., Wang, L., Shi, F., Gilmore, J. H., Lin, W., & Shen, D. (2015). Construction of 4D high-definition cortical surface atlases of infants: Methods and applications. *Medical Image Analysis*, *25*(1), 22–36.

Luders, E., Narr, K., Thompson, P., Rex, D., Jancke, L., & Toga, A. (2005). Hemispheric asymmetries in cortical thickness. *Cerebral Cortex*, *16*(8), 1232–1238.

Lyall, A. E., Shi, F., Geng, X., Woolson, S., Li, G., Wang, L., … Gilmore, J. H. (2014). Dynamic development of regional cortical thickness and surface area in early childhood. *Cerebral Cortex*, *25*(8), 2204–2212. https://doi.org/10.1093/cercor/bhu027%J

Lyn, H., Pierre, P., Bennett, A. J., Fears, S., Woods, R., & Hopkins, W. D. (2011). Planum temporale grey matter asymmetries in chimpanzees (*Pan troglodytes*), vervet (*Chlorocebus aethiops* sabaeus), rhesus (*Macaca mulatta*) and bonnet (*Macaca radiata*) monkeys. *Neuropsychologia*, *49*(7), 2004–2012.

Lyttelton, O. C., Karama, S., Ad-Dab'bagh, Y., Zatorre, R. J., Carbonell, F., Worsley, K., & Evans, A. C. (2009). Positional and surface area asymmetry of the human cerebral cortex. *NeuroImage*, *46*(4), 895–903.

Malkova, L., Heuer, E., & Saunders, R. (2006). Longitudinal magnetic resonance imaging study of rhesus monkey brain development. *European Journal of Neuroscience*, *24*(11), 3204–3212.

Marie, D., Roth, M., Lacoste, R., Nazarian, B., Bertello, A., Anton, J.-L., … Meguerditchian, A. (2017). Left brain asymmetry of the Planum Temporale in a nonhominid primate: Redefining the origin of brain specialization for language. *Cerebral Cortex*, *28*(5), 1808–1815.

Mesulam, M.-M. (1998). From sensation to cognition. *Brain: A Journal of Neurology*, *121*(6), 1013–1052.

Muntané, G., Santpere, G., Verendeev, A., Seeley, W. W., Jacobs, B., Hopkins, W. D., … Sherwood, C. C. (2017). Interhemispheric gene expression differences in the cerebral cortex of humans and macaque monkeys. *Brain Structure and Function*, *222*(7), 3241–3254.

Nie, J., Li, G., Wang, L., Gilmore, J. H., Lin, W., & Shen, D. (2011). A computational growth model for measuring dynamic cortical development in the first year of life. *Cerebral Cortex*, *22*(10), 2272–2284.

Niu, Y., Li, T., & Ji, W. (2017). Paving the road for biomedicine: Genome editing and stem cells in primates. *National Science Review*, *4*(4), 543–549.

Ochiai, T., Grimault, S., Scavarda, D., Roch, G., Hori, T., Riviere, D., … Régis, J. (2004). Sulcal pattern and morphology of the superior temporal sulcus. *NeuroImage*, *22*(2), 706–719.

Panizzon, M. S., Fennema-Notestine, C., Eyler, L. T., Jernigan, T. L., Prom-Wormley, E., Neale, M., … Kremen, W. S. (2009). Distinct genetic influences on cortical surface area and cortical thickness. *Cerebral Cortex*, *19*(11), 2728–2735. https://doi.org/10.1093/cercor/bhp026%J

Rilling, J. K. (2014). Comparative primate neuroimaging: Insights into human brain evolution. *Trends in Cognitive Sciences*, *18*(1), 46–55.

Scott, J. A., Grayson, D., Fletcher, E., Lee, A., Bauman, M. D., Schumann, C. M., … Amaral, D. G. (2016). Longitudinal analysis of the developing rhesus monkey brain using magnetic resonance imaging: Birth to adulthood. *Brain Structure and Function*, *221*(5), 2847–2871.

Shaw, P., Lalonde, F., Lepage, C., Rabin, C., Eckstrand, K., Sharp, W., … Rapoport, J. (2009). Development of cortical asymmetry in typically developing children and its disruption in attention-deficit/hyperactivity disorder. *Archives of General Psychiatry*, *66*(8), 888–896.

Sun, L., Zhang, D., Wang, L., Shao, W., Chen, Z., Lin, W., … Li, G. (2018). Topological correction of infant cortical surfaces using anatomically constrained U-net. *Paper presented at the International Workshop on Machine Learning in Medical Imaging*.Springer.

Thompson, P., Moussai, J., Zohoori, S., Goldkorn, A., Khan, A., Mega, M., … Toga, A. (1998). Cortical variability and asymmetry in normal aging and Alzheimer's disease. *Cerebral Cortex (New York, NY: 1991)*, *8*(6), 492–509.

Toga, A. W., Thompson, P. M. (2003). Mapping brain asymmetry. *Nat RevNeurosci*. *4*, 37–48.

Van Essen, D. C. (2005). A population-average, landmark-and surface-based (PALS) atlas of human cerebral cortex. *NeuroImage*, *28*(3), 635–662.

Van Essen, D. C., Glasser, M. F., Dierker, D. L., Harwell, J., & Coalson, T. (2011). Parcellations and hemispheric asymmetries of human cerebral cortex analyzed on surface-based atlases. *Cerebral Cortex*, *22*(10), 2241–2262.

Wang, F., Lian, C., Xia, J., Wu, Z., Duan, D., Wang, L., … Li, G. (2018). Construction of spatiotemporal infant cortical surface atlas of rhesus macaque. *2018 IEEE 15th International Symposium on Biomedical Imaging. Paper presented at the Biomedical Imaging (ISBI 2018)*. IEEE.

Wang, L., Gao, Y., Shi, F., Li, G., Gilmore, J. H., Lin, W., & Shen, D. (2015). LINKS: Learning-based multi-source IntegratioN frameworK for segmentation of infant brain images. *NeuroImage*, *108*, 160–172.

Wang, L., Shi, F., Li, G., Gao, Y., Lin, W., Gilmore, J. H., & Shen, D. (2014). Segmentation of neonatal brain MR images using patch-driven level sets. *NeuroImage*, *84*, 141–158.

Wang, L., Shi, F., Yap, P. T., Lin, W., Gilmore, J. H., & Shen, D. (2013). Longitudinally guided level sets for consistent tissue segmentation of neonates. *Human Brain Mapping*, *34*(4), 956–972.

Watson, K. K., & Platt, M. L. (2012). Of mice and monkeys: Using non-human primate models to bridge mouse-and human-based investigations of autism spectrum disorders. *Journal of Neurodevelopmental Disorders*, *4*(1), 21.

Worsley, K. J., Taylor, J. E., Tomaiuolo, F., Lerch, J. (2004). Unified univariate and multivariate random field theory. *Neuroimage*, *23*(Suppl 1), S189–S195.

Worsley, K. J., Taylor, J. E., Carbonell, F., Chung, M., Duerden, E., Bernhardt, B., … Evans, A. (2009). SurfStat: A Matlab toolbox for the

statistical analysis of univariate and multivariate surface and volumetric data using linear mixed effects models and random field theory. *NeuroImage*, *47*, S102.

Xia, J., Wang, F., … Gang, L. (2018). A computational method for longitudinal mapping of orientation-specific expansion of cortical surface in infants. *Medical Image Analysis*, *49*, 46–59.

Yeo, B. T., Sabuncu, M. R., Vercauteren, T., Ayache, N., Fischl, B., & Golland, P. (2010). Spherical demons: Fast diffeomorphic landmark-free surface registration. *IEEE Transactions on Medical Imaging*, *29*(3), 650–668.

Young, J. T., Shi, Y., Niethammer, M., Grauer, M., Coe, C. L., Lubach, G. R., … Alexander, A. L. (2007). The UNC-Wisconsin rhesus macaque neurodevelopment database: A structural MRI and DTI database of early postnatal development. *Frontiers in Neuroscience*, *11*, 29.

SUPPORTING INFORMATION

Additional supporting information may be found online in the Supporting Information section at the end of this article.

How to cite this article: Xia J, Wang F, Wu Z, et al. Mapping hemispheric asymmetries of the macaque cerebral cortex during early brain development. *Hum Brain Mapp*. 2020;41: 95–106. https://doi.org/10.1002/hbm.24789